

**Technical Paper by R.M. Koerner, G.R. Koerner and
M.A. Eberlé**

OUT-OF-PLANE TENSILE BEHAVIOR OF GEOSYNTHETIC CLAY LINERS

ABSTRACT: Presented in this paper is the out-of-plane tensile behavior of a variety of geosynthetic clay liners (GCLs). Tensile response curves indicate that GCL strength is largely dependent on the carrier material types from which the GCL is manufactured. Fiber reinforcement effects as well as orientation effects were relatively small for this type of test. The effects of hydration and seams were also assessed. The study shows that GCLs can withstand considerably greater out-of-plane deformation than compacted clay liners (CCLs). Review of the results indicates that GCLs should be considered over CCLs for use as barrier layers where differential subsidence is anticipated.

KEYWORDS: Geosynthetic clay liners, Out-of-Plane deformation, Subsidence behavior, Laboratory testing, Three-Dimensional axi-symmetric tension test.

AUTHORS: R.M. Koerner, H.L. Bowman Professor of Civil Engineering and Director - GRI, G.R. Koerner, Research Assistant Professor, and M.A. Eberlé, Graduate Student, Drexel University, Geosynthetic Research Institute, Philadelphia, Pennsylvania 19104, USA, Telephone: 1/215- 895-2343, Telefax: 1/215-895-1437.

PUBLICATION: *Geosynthetics International* is published by the Industrial Fabrics Association International, 345 Cedar St., Suite 800, St. Paul, Minnesota 55101, USA, Telephone: 1/612-222-2508, Telefax: 1/612-222-8215. *Geosynthetics International* is registered under ISSN 1072-6349.

DATES: Original manuscript received 21 November 1995, revised version received 2 April 1996 and accepted 3 April 1996. Discussion open until 1 November 1996.

REFERENCE: Koerner, R.M., Koerner, G.R and Eberlé, M.A., 1996, "Out-of-Plane Tensile Behavior of Geosynthetic Clay Liners", *Geosynthetics International*, Vol. 3, No. 2, pp. 277-296.

1 INTRODUCTION

There are numerous situations where the tensile strength of landfill liner materials, such as geomembranes, compacted clay liners (CCLs) and geosynthetic clay liners (GCLs), is mobilized in an out-of-plane mode of deformation. One situation is that of a landfill cover where the underlying waste may undergo differential settlement over time due to densification and decomposition. This subsidence can take place in a localized area which requires the liner system above it to deform in an out-of-plane mode.

Past research using the ASTM D 5617 standard test method for multi-axial tension testing has shown that geomembranes perform reasonably well in an out-of-plane deformation mode with the following strains at failure for geomembranes currently available (Koerner et al. 1990):

- reinforced chlorosulphonated polyethylene (CSPE-R) \cong 10%;
- high density polyethylene (HDPE) \cong 20%;
- polyvinyl chloride (PVC) \cong 75%;
- linear low density polyethylene (LLDPE) \cong 75%; and
- very low density polyethylene (VLDPE) \cong 100%.

While a geomembrane can be used by itself in a landfill cover it is most commonly used in combination with an underlying clay in composite liner systems. Such composite liners are required by federal and state regulations in many countries, e.g. USA and Germany.

When the clay component of the composite liner system is a CCL, differential settlement cannot be accommodated to any great extent. For example, CCLs fail by tensile cracking at strains much less than 1% (Koerner and Daniel 1994). Table 1 shows that the failure tensile strain for clay soils varies from 0.07 to 0.84% when evaluated in a beam splitting test configuration. Only with pure bentonite does the strain value increase to 3.4%. However, to the best of the authors' knowledge, this material is never used as the sole barrier material due to its unacceptably low hydrated shear strength.

Table 1. Data on tensile strain at failure for compacted clay (LaGatta 1992).

Type or source of soil	Water content (%)	Plasticity index* (%)	Tensile strain at failure (%)
Natural clayey soil	19.9	7	0.80
Illite	31.5	34	0.84
Kaolinite	37.6	38	0.16
Portland Dam	16.3	8	0.14
Rector Creek Dam	19.8	16	0.10
Woodcrest Dam	10.2	Non-plastic	0.18
Shell Oil Dam	11.2	Non-plastic	0.07
Willard Test Embankment	16.4	11	0.20
Bentonite	101	487	3.4

Note: *Defined as the liquid limit minus the plastic limit (ASTM D 4318).

In the authors' opinion, to use a CCL as the lower clay component of a composite liner (much less by itself) is essentially futile in the case of localized subsidence of a landfill cover. A different type of clay liner should be considered if out-of-plane deformation is anticipated, such as a GCL. However, the quantification of the amount of out-of-plane tensile deformation of a GCL in a landfill cover must be established.

In addition to landfill cover applications, the following cases require quantification of the out-of-plane tensile behavior of a GCL:

- GCLs placed over differentially subsiding soil subgrades;
- GCLs placed over karst topography;
- GCLs placed over thermokarst topography;
- GCLs placed in areas sensitive to mining subsidence;
- GCLs placed over rock subgrades (either non-backfilled or partially backfilled);
- GCLs placed over backfilled pipelines where settlement is possible; and
- GCLs placed over tunnels where backfill settlement is possible.

This paper is focused on the three-dimensional, axi-symmetric tension test (ASTM D 5617) that was used to provide data for ten commercially available GCLs. Both the raw data and calculated stress versus strain data are presented.

To the authors' knowledge, the only other comparable data available in the open literature is the work of LaGatta (1992) and Boardman (1993) at the University of Texas in Austin. By using large rectangular containers and controlling subsidence via removal of water from an underlying diaphragm, they evaluated hydraulic conductivity with respect to the deformation of different GCLs. The amount of subsidence at which the hydraulic conductivity began to increase was defined as the limiting allowable distortion. LaGatta (1992) and Boardman (1993) reported that many GCLs could withstand distortion ratios (i.e. vertical deformation, δ , divided by the radius of deformation, $L/2$, of up to $\delta/(L/2) = 0.5$. This relates to an approximate tensile strain in the deflected GCL of 10 to 15%. While hydraulic conductivity is quite different from the focus of this study on out-of-plane tensile behavior, the results of the work of LaGatta (1992) and Boardman (1993) should be kept in mind.

2 TEST APPARATUS

The laboratory tests in the current study were conducted in a relatively large pressure vessel 0.6 m in diameter with the cross section shown in Figure 1. In conducting such a test, a circular GCL test specimen was placed over the flange of the lower assembly and a 1.0 mm thick VLDPE geomembrane was placed directly above it. (Alternatively, other very flexible geomembranes could have been used.) The purpose of the geomembrane was to: contain the hydrostatic pressure applied to it and the underlying GCL specimen; prevent hydration of the GCL specimen; and prevent water flow through the GCL specimen. The tensile resistance of the VLDPE geomembrane was deducted from the composite VLDPE/GCL response as described below.

The upper pressure vessel assembly was placed above the VLDPE geomembrane and the upper and lower assemblies were clamped together making a water tight seal. A

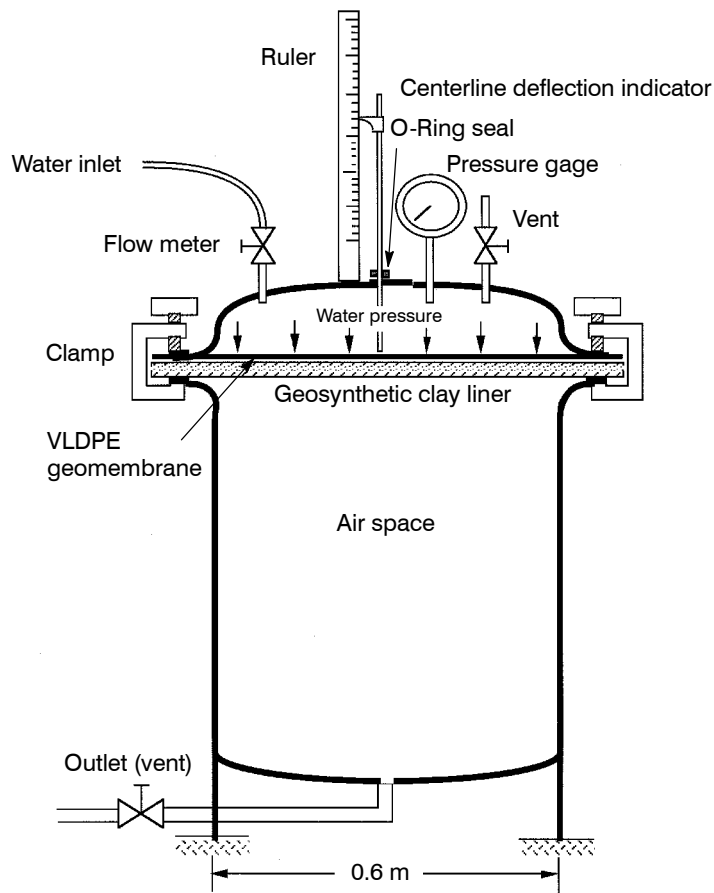


Figure 1. Pressure vessel setup.

centerline deflection indicator in contact with the top of the geomembrane and a ruler were used to measure deflections. Water was then introduced until the upper assembly was purged of air. The upper assembly vent was closed and water was introduced at the rate 1.9 L/min which resulted in a 7.0 kPa per minute pressure rate (ASTM D 5617). As the hydrostatic pressure was increased, the VLDPE/GCL composite deformed into the empty lower assembly. The lower assembly vent was always kept open. Centerline deflection and pressure readings were taken manually at regular intervals throughout the test. Eventually, the GCL specimen failed in an abrupt manner (failure was readily observed on the pressure gauge, and witnessed audibly). As anticipated, the VLDPE geomembrane did not fail in any of these tests due to its high extensibility with respect to that of the GCL specimens.

During the course of this study, ten different GCLs produced by five manufacturers were tested. The GCLs evaluated were made using a variety of woven and nonwoven geotextiles, and textured and smooth HDPE geomembranes, in combination with vari-

ous forms of bentonite, i.e. powdered and granular. The GCLs were either adhesive bonded, stitch-bonded or needle-punched to the geotextiles or geomembranes. Table 2 describes the different GCLs used in the test program. The thicknesses were measured at a normal stress of 2.0 kPa and are reported as the average of ten measurements. There are numerous references available on the different types and styles of GCLs (Koerner et al. 1994).

Two different types of GCL-A were tested in this study. The first consists of sodium activated bentonite powder sandwiched between two needle-punched nonwoven geotextiles, the lower one being scrim reinforced. The second consists of sodium bentonite encapsulated between a needle-punched nonwoven and a slit-film woven geotextile. For both types of GCL-A, fibers from the upper nonwoven geotextile are needle-punched through the bentonite and lower geotextile. The dangling fibers are then heat fused to the lower geotextile to form GCL-A2.

The manufacturing process for GCL-B involves the placement of sodium bentonite granules between two polypropylene geotextiles. The upper geotextile is a needle-punched nonwoven and the lower geotextile is a slit-film woven. The fibers from the upper geotextile are needle-punched through the clay and lower geotextile. The fibers are then bonded to the outer surface of the woven geotextile by the application of an adhesive bonding agent.

GCL-C consists of sodium-activated bentonite powder sandwiched between two knitted geotextiles. There is an additional thin geotextile layer in the center. The composite is completed by stitching all three layers together in the machine direction at 25 mm spacings.

Table 2. Description of the different GCL products evaluated.

GCL No.	Upper surface	Lower surface	Bentonite type	Mechanical structure	Thickness** (mm)
A1	NPNW-GT	NPNW-GT	Na* powder	Needle-punched	7.0
A2	NPNW-GT	NPNW-GT	Na powder	Needle-punched	5.9
B	NPNW-GT	SFW-GT	Na granules	Needle-punched	5.3
C	K-GT	K-GT	Na* powder	Stitch-bonded	5.0
D1	SFW-GT	SFW-GT	Na granules	Adhesive	5.0
D2	SFW-GT	SFW-GT	Na granules	Stitch-bonded	5.0
D3	SFW-GT	SFW-GT	Na granules	Stitch-bonded	4.9
E1	none	HDPE-GM(s)	Na granules	Adhesive	4.6
E2	HBNW-GT	HDPE-GM(s)	Na granules	Adhesive	4.5
E3	none	HDPE-GM(t)	Na granules	Adhesive	4.6

Notes: NPNW-GT = needle-punched nonwoven geotextile; SFW-GT = slit-film woven geotextile; HBNW-GT = heat-bonded nonwoven geotextile; K-GT = knitted geotextile; HDPE-GM(s) = high density polyethylene geomembrane (smooth); HDPE-GM(t) = high density polyethylene geomembrane (textured); Na = sodium; Na* = activated sodium. **Thickness as per ASTM D 5199.

Three types of GCL-D were tested in this study. They consist of granular sodium bentonite adhesively bonded between an upper and lower geotextile. In all cases, the geotextiles are slit-film woven types but with different construction. For example, the slit-film yarns in GCL-D3 are in both the machine and cross-machine directions, while in GCL-D1 and GCL-D2 the slit-film yarns are in the machine direction only. The GCL-D1 is not stitch-bonded, while GCL-D2 and GCL-D3 are stitch-bonded with a heavy sewing yarn between the upper and lower geotextiles in the machine direction at 100 mm spacings.

GCL-E is manufactured by adhesively bonding bentonite granules to an HDPE geomembrane. (Other geomembranes, either smooth or textured, could also be used.) Three different types of geomembrane were tested: GCL-E1 with a smooth HDPE geomembrane on one side; GCL-E2 with a different smooth HDPE geomembrane on one side and a very light nonwoven geotextile placed over the bentonite; and GCL-E3 with a textured HDPE geomembrane on one side.

It should be recognized that all of these GCLs are subject to change and the manufacturers should be consulted for the current composition of their products.

3 DATA PRESENTATION

The three-dimensional, axi-symmetric tension test method used in this study is regularly performed on geomembranes (ASTM D 5617). The test is somewhat controversial in the method of data presentation. The approach for handling the raw data is straightforward since one can readily plot the measured applied pressure versus centerpoint deflection data until the test specimen fails. At issue is the manipulation of the data to arrive at corresponding stress versus strain data. The latter is clearly desirable from an engineering perspective. In order to provide such information one must assume the incremental shape of the test specimen as it deforms during the test and eventually fails. This is clearly a complex situation. While deforming into the lower assembly as shown in Figure 1, the central portion of the test specimen likely deforms more than the region near the clamps (Steffen 1984). This is quite pronounced near failure and upon removing the test specimen the central section is always seen to be greatly distorted. It is quite possible that the deformation is nonlinear from the center to the edge resulting in a difficult stress state and consequently a complex system to analyze.

To simplify the calculation of strain (in accordance with ASTM D 5617) it was assumed that the deformed shape of the test specimen is hemispherical with a gradually downward moving center. This assumption was used at least up to a centerpoint deformation equal to the radius of the test specimen. For all of the GCL tests, failure occurred before this deformation limit was reached. Using this assumption, the analysis is straightforward. The complete analytical derivation is described in the GRI GM4 test method and is used in the ASTM D 5617 test procedure.

To obtain the strain for a centerpoint deflection of $\delta < L/2$, the GCL test specimen is assumed to deform into the segment of a circle as shown in Figure 2.

Using geometric relationships (GRI GM4), the geosynthetic tensile strain, ϵ , can be calculated utilizing the following equations:

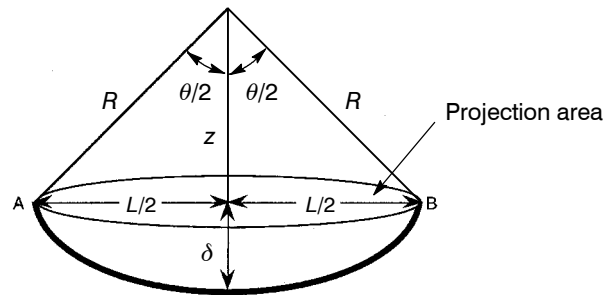


Figure 2. The original projection area for the calculation of the applied pressure to GCL specimens in the test apparatus (GRI GM4; ASTM D 5617).

$$R = \frac{L^2 + 4\delta^2}{8\delta} \quad (1)$$

$$\theta = 2 \tan^{-1} \frac{4L\delta}{L^2 - 4\delta^2} \quad (2)$$

$$\text{arc length (AB)} = R\theta \quad (3)$$

$$\varepsilon = \frac{\text{arc length (AB)} - L}{L} (100) \% \quad (4)$$

where: R = radius; δ = centerpoint deflection; θ = angle between two radii which connect to the perimeter of the geomembrane specimen (radians); and z = vertical distance from the origin of the arc to the horizontal chord AB.

From Figure 2 it can be seen that when $\delta = 0$, then $R = \infty$, $\theta = 0^\circ$ and chord AB = L .

To obtain the stress associated with the above strain for a centerpoint deflection of $\delta < L/2$, the applied pressure acts over the original projection area (Figure 2). Taking a force summation in the vertical direction yields the value of stress, σ (GRI GM4):

$$\sigma = \frac{Lp}{4t \sin(\theta/2)} \quad (5)$$

where: t = geomembrane thickness; p = applied pressure; and θ = angle between two radii which connect to the perimeter of the geomembrane specimen (radians).

Using Equations 1, 2, 3 and 4 sequentially results in strain values for various deflection readings. These values are then coupled with the results of Equation 5 which gives the value of stress for a given pressure reading. The two sets of values allow stress versus strain response curves to be plotted for the test.

4 EXPERIMENTAL RESULTS

Before describing the experimental results of the various GCL specimens, two preliminary sets of results are presented. One is a series of replicate tests on the same type of GCL specimens to determine the repeatability of the test and the other is the method for elimination of the VLDPE geomembrane strength contribution to calculate the desired GCL specimen response.

Following these two sets of experiments, the test results for the GCL specimens described in Table 2 are presented. Due to the acknowledged controversy of the previous analytic formulation, however, both pressure versus deflection (i.e. raw data) and stress versus strain (i.e. calculated data) plots are presented.

4.1 Repeatability Tests

A series of five tests were conducted on GCL-A2 specimens to determine the repeatability of the test method. The results of the raw data are shown in Figure 3. Initially a concave region is seen, which is indicative of a gradual tightening of the GCL specimen and geomembrane, as well as seating of the test specimen within the clamped edges. A relatively linear response is seen thereafter. In all cases, failure was very abrupt and accompanied by an audible sound. At the same time, a rapid decrease in pressure was observed as the VLDPE geomembrane “protruded through” the failed GCL specimen. The average hydrostatic pressure at failure was 129 kPa, with a standard deviation of 10.7 kPa (coefficient of variation of 8.3%). The average centerpoint deflection at failure was 180 mm, with a standard deviation of 11 mm (coefficient of variation of 6.5%). These values seem reasonable based on the experience of the authors with the statistical variation of results from other geosynthetic (and geotechnical) test methods.

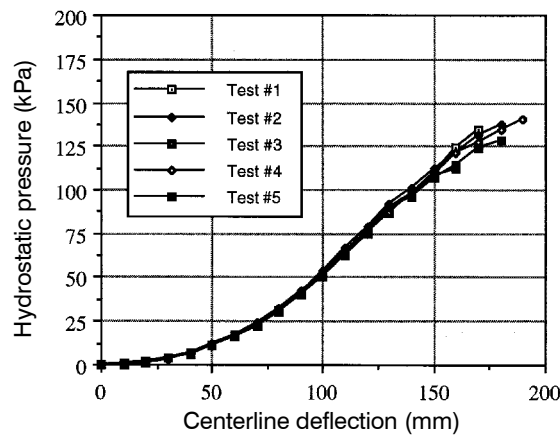


Figure 3. Repeat tests for GCL-A2 specimens.

4.2 Elimination of VLDPE Response

In order to separate the strength contribution of the VLDPE geomembrane from the strength of the GCL specimen, the hydrostatic pressure versus centerpoint deflection curve for the VLDPE geomembrane used in the tests was subtracted from the curve for the combined VLDPE/GCL response. In theory, this simple curve subtraction should produce a curve representative of the behavior of the GCL specimen alone.

This assumption was challenged by testing GCL-E1 specimens with and without the additional VLDPE geomembrane. Testing GCL-E1 specimens without the additional VLDPE geomembrane was possible because GCL-E1 includes an attached HDPE geomembrane. From the testing of GCL-E1 specimens with the additional VLDPE geomembrane, the calculated hydrostatic pressure versus centerpoint deflection curve for GCL-E1 specimens alone was obtained by subtracting the curve for the VLDPE geomembrane alone from the combined VLDPE/GCL-E1 curve as shown in Figure 4. Comparing the curve achieved by subtraction to the actual curve of the GCL-E1 specimen alone shows that the curves exhibit almost identical behavior up until the failure of the GCL-E1 specimen. The failure was prolonged, however, by testing with the additional VLDPE geomembrane. Due to this very close correlation it is felt that subtraction of the VLDPE geomembrane response is valid for the purposes of this study. This technique was used throughout this study and only the isolated GCL specimen response curves are reported in Figures 5 to 12.

4.3 GCL-A Response

The response curves for the two GCL-A products evaluated are shown in Figures 5a and 5b. Note that the product with the fibers fused to the lower geotextile (GCL-A2 specimens) gave a slightly stiffer response in the raw data than the nonfused product (GCL-A1 specimens). As a result of converting the raw data to stress versus strain data, the responses are slightly exaggerated but maintain their relative positions.

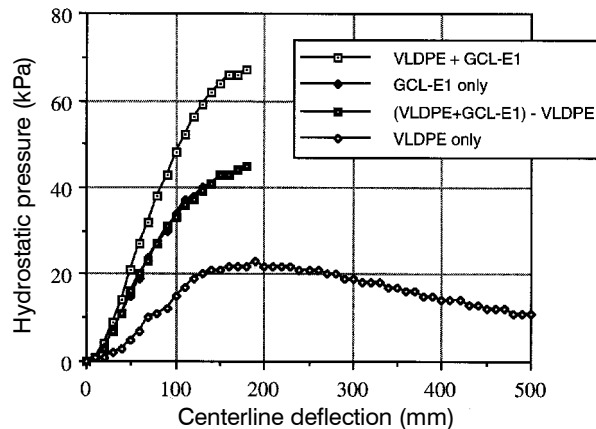


Figure 4. Method of elimination of VLDPE geomembrane strength contribution to composite VLDPE/GCL strength response.

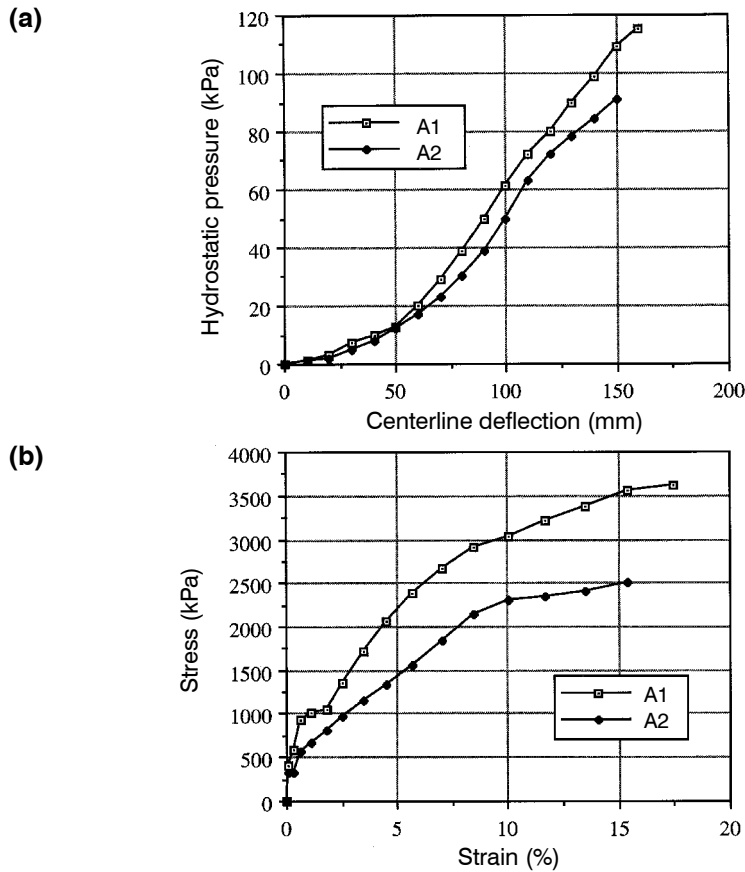


Figure 5. Comparison of test results for GCL-A1 and GCL-A2 specimens (fibers not fused to the lower geotextile and fibers fused, respectively): (a) raw data; (b) calculated stress versus strain data.

The product with heat fused fibers (GCL-A1 specimens) was further evaluated to determine if differences occur with respect to the orientation of the product during placement. Shown in Figures 6a and 6b are the response curves obtained with the fused fibers side up, and down. It is seen that a slight stiffening effect results from placing the fused fiber side down, which is understandable since the tensile stresses are greatest on the bottom surface of the composite test cross section; however, the difference is very small. The mode of failure in this set of tests was a centralized tear in the cross-machine direction of the lower geotextile.

4.4 GCL-B Response

GCL-B specimens were evaluated with the slit-film woven geotextile facing up and down. The raw data response curves are almost identical (Figure 7a). The response is

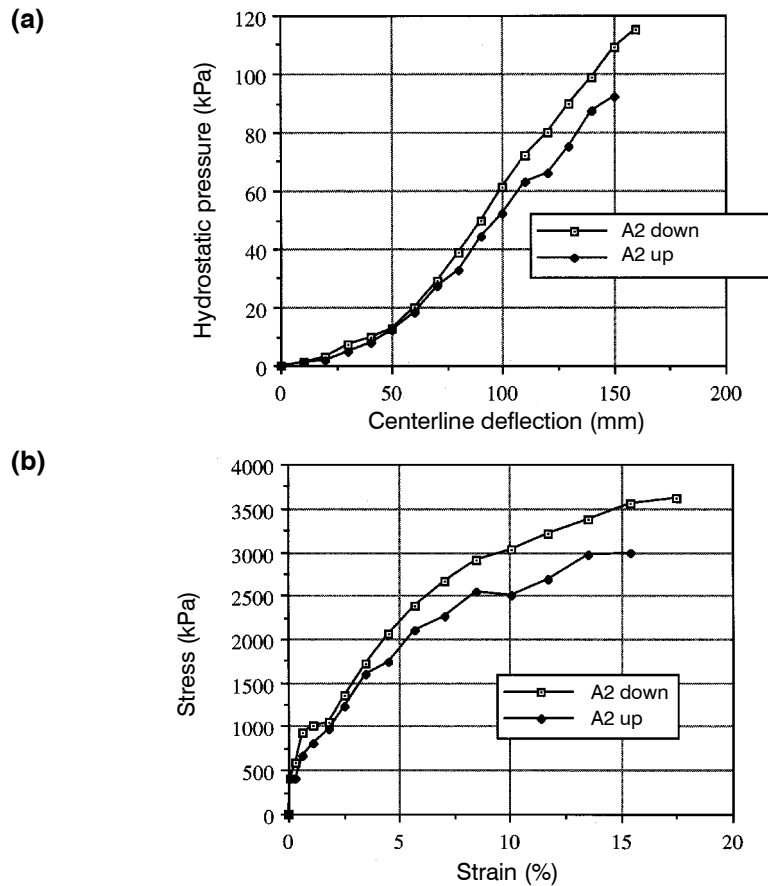


Figure 6. Comparison of test results for heat fused side up and down for GCL-A2 specimens: (a) raw data; (b) calculated stress versus strain data.

similar for the stress versus strain curves in Figure 7b. However, failure with the slit-film side down occurred at a slightly lower deflection (and strain) than with the needle-punched nonwoven side down. This is understandable due to the relatively lower strain at failure behavior of the slit-film woven geotextile in comparison to that of the needle-punched nonwoven geotextile. The mode of failure for both the slit-film woven geotextile facing up and down was by a centralized “T-shaped” tear of the lower geotextile.

4.5 GCL-C Response

The response of the three geotextile layer, stitch-bonded, GCL-C specimens was somewhat unique in comparison to the other GCL specimens. Figures 8a and 8b show the response curves for the raw data and the calculated stress versus strain, respectively. Here one observes a relatively large deflection of 100 mm (strain of approximately 6%), at a relatively low pressure and stress. This response could be attributed to the removal

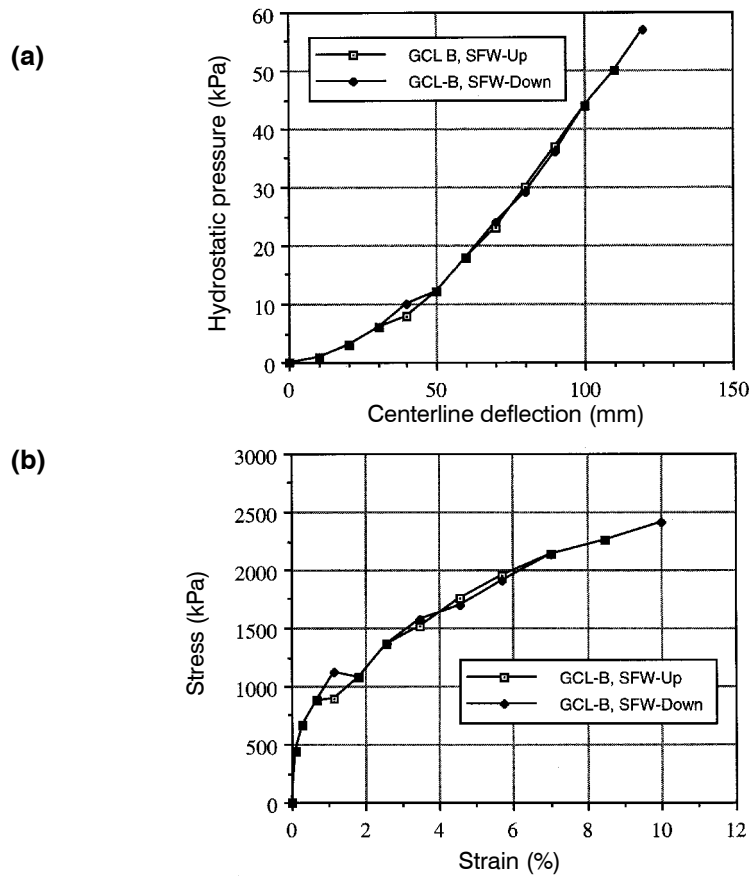


Figure 7. Comparison of test results for GCL-B with the slit-film woven geotextile facing up and down: (a) raw data; (b) calculated stress versus strain data.

of slack within the three layers of geotextile which is unique to this product. When all three layers act together the response is more typical of the other GCL specimens tested. It should be noted that GCL specimen failure (by tearing) always occurred perpendicular to the stitch-bonded rows of the geotextiles.

4.6 GCL-D Response

The response for the different GCL-D products tested is shown in Figures 9a and 9b. As would be expected, the non-stitch-bonded GCL-D1 specimen exhibits slightly greater elongation at lower stresses than its stitch-bonded counterparts; however, the responses at failure were essentially the same. The two response curves for GCL-D2 and GCL-D3 specimens were from different styles of the product which had slightly different carrier layer geotextiles. These products had failure strain differences of approximately 10% which can be attributed to the variation in geotextile construction.

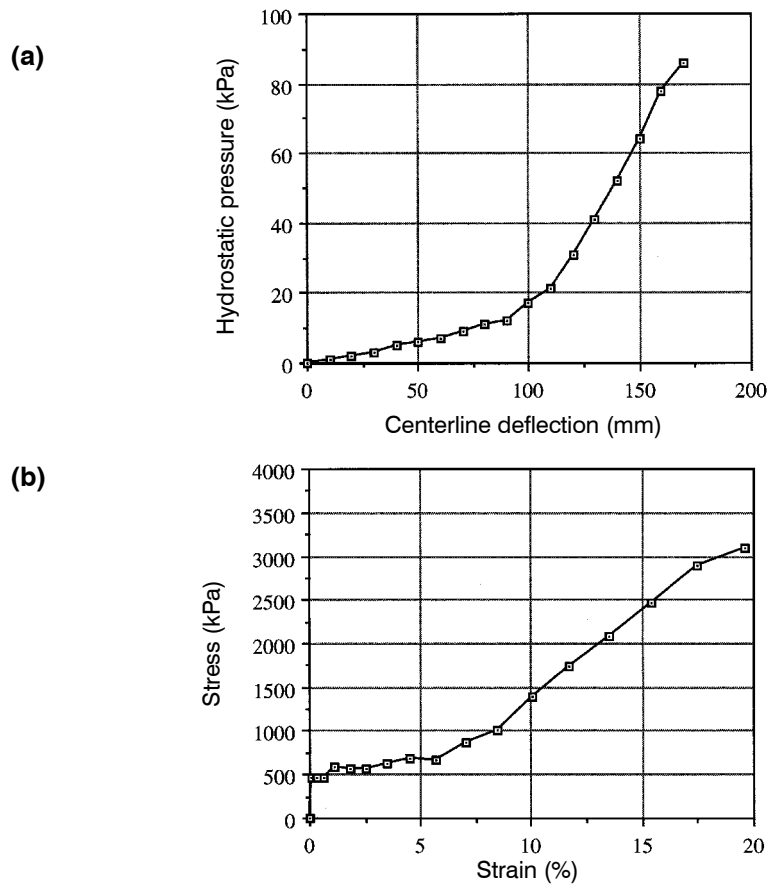


Figure 8. GCL-C specimens: (a) raw data; (b) calculated stress versus strain data.

Failure of the stitch-bonded GCL specimens (by tearing) occurred in a direction parallel to the rows of stitching of the geotextiles. To evaluate the influence of seams for this mode of testing additional GCL-D1 specimens were tested (Section 4.9).

4.7 GCL-E Response

All three GCL-E products were initially tested with the bentonite side facing down. The response curves are shown in Figures 10a and 10b. There appear to be differences in the pressure versus centerpoint deflection, which were accentuated in the stress versus strain response. The curves plotted in the stress versus strain format appear quite similar to HDPE geomembrane response curves in the same type of test (Koerner et al. 1990). The GCL-E2 product was also tested with the bentonite side up. It resulted in a surprisingly lower pressure and stress at failure, and an expected larger deflection and strain at failure. The mode of failure in all cases was a tear through the central region of the geomembrane.

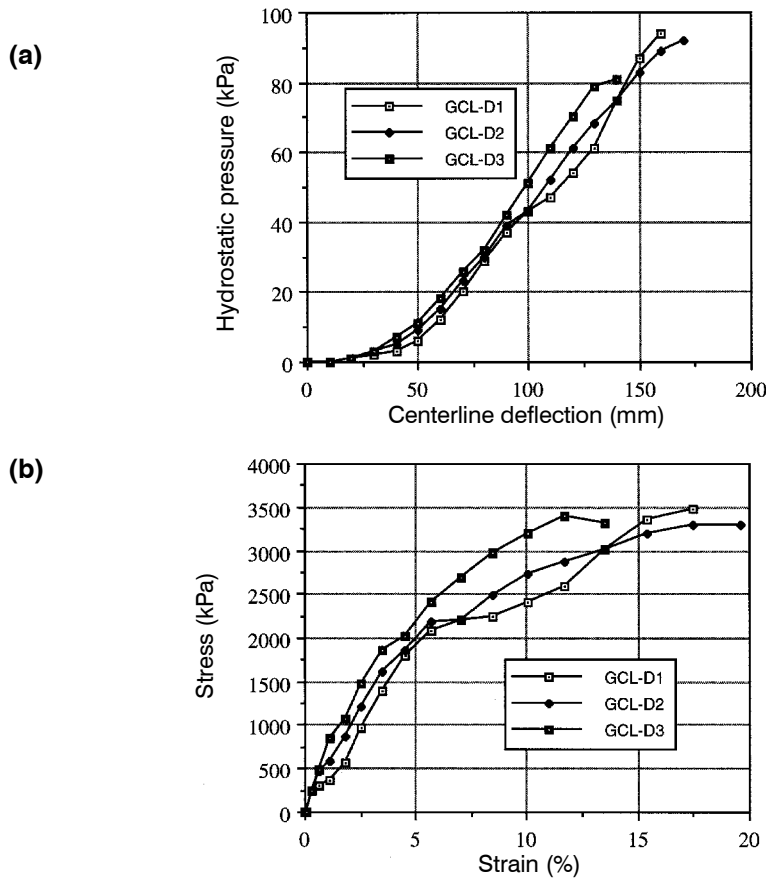


Figure 9. Comparison of test results for stitch-bonded (GCL-D2 and GCL-D3) and non-stitch-bonded (GCL-D1) GCL specimens: (a) raw data; (b) calculated stress versus strain data.

4.8 Effect of Bentonite Hydration

It should be noted that all of the tests presented thus far used the GCL specimens in an “as received” moisture condition. While this is usually referred to as the “dry” condition, there is actually some moisture present due to the adsorption characteristics of bentonite. This amount of moisture depends on the type of bentonite, particle size of the bentonite, exposure to the atmosphere, and the relative humidity of the local environment. The moisture content varied between 10 and 20% with the higher value being associated with the adhesively bonded products.

In the field, however, there is a concern with respect to the three-dimensional, axisymmetric behavior in the fully hydrated state. To evaluate this situation a sample of

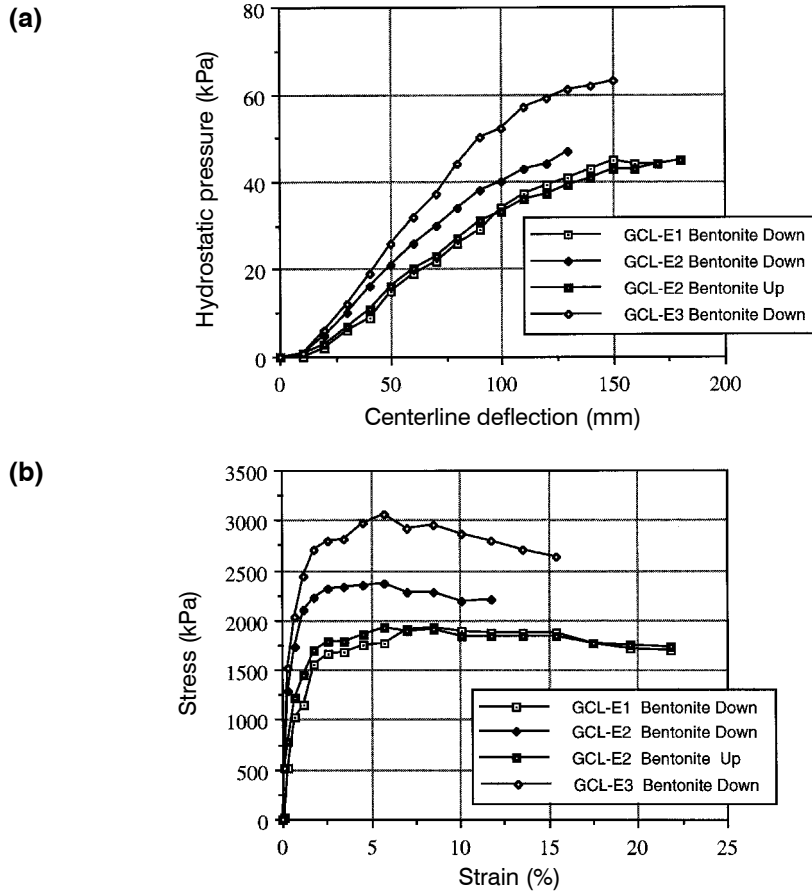


Figure 10. Comparison of test results for GCL-E specimens: (a) raw data; (b) calculated stress versus strain data.

GCL-A1 was evaluated in its dry versus hydrated states. The actual moisture contents were 10 and 280%, respectively.

The response curves for the dry and hydrated GCL specimens are presented in Figures 11a and 11b. It can be seen that the initial response of the hydrated GCL specimen followed the dry specimen closely up to an approximate 70 mm deflection. Thereafter, however, the hydrated specimen had lower strength and the response curves began to deviate. At 120 mm deflection, the hydrated specimen response curve dropped sharply. This may have been due to movement of the hydrated bentonite within the test specimen, i.e. a lateral squeezing effect. The test was repeated three times with essentially the same results. The stress versus strain response is an exaggerated version of the pressure versus deflection curves.

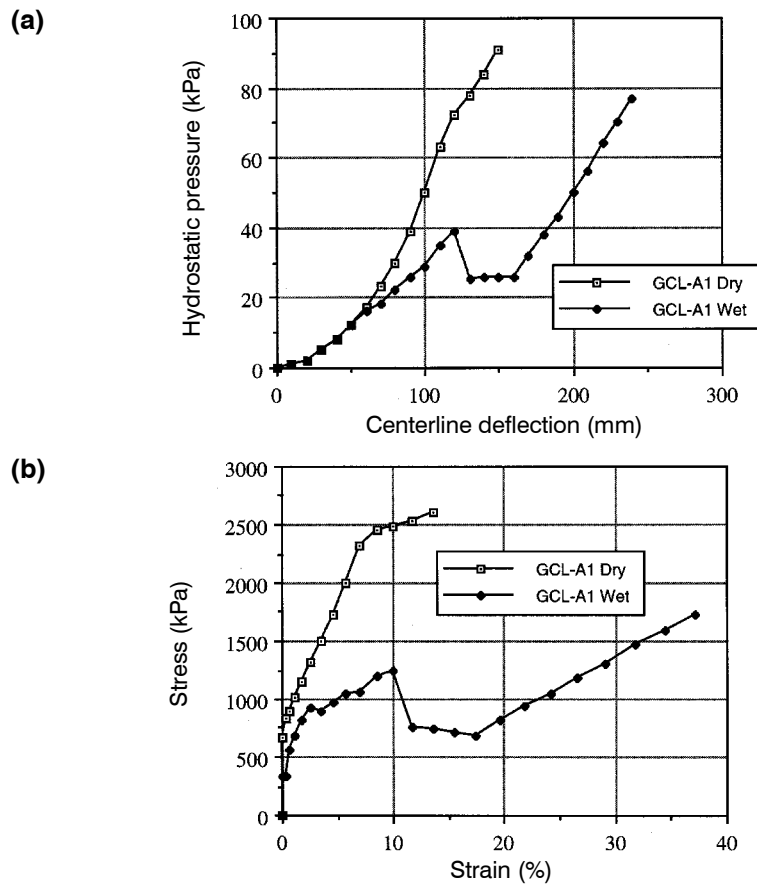


Figure 11. Comparison of test results of GCL-A1 specimen in dry and hydrated states: (a) raw data; (b) calculated stress versus strain data.

4.9 Effect of Overlap Seams

The response of differential settlement on GCL strength behavior presented thus far has been on full test specimens without overlaps. However, the edges and ends of GCL rolls in the field must be overlapped and differential settlement could possibly occur beneath such overlaps. To address this issue, a series of tests was conducted using GCL-D1 specimens with a range of overlap seam distances. The response curves for specimens with 100, 150, 200 and 250 mm seam overlap distances are shown in Figures 12a and 12b together with an intact GCL specimen without a seam. All seam tests show stiffer responses than the test specimen without a seam. Furthermore, the greater the overlap, the greater the resulting stiffness. The greater stiffness is likely due to the double thickness of the GCL in the overlapped region as compared to the calculated response of a single thickness of GCL. Additionally, the rounded test specimen configuration

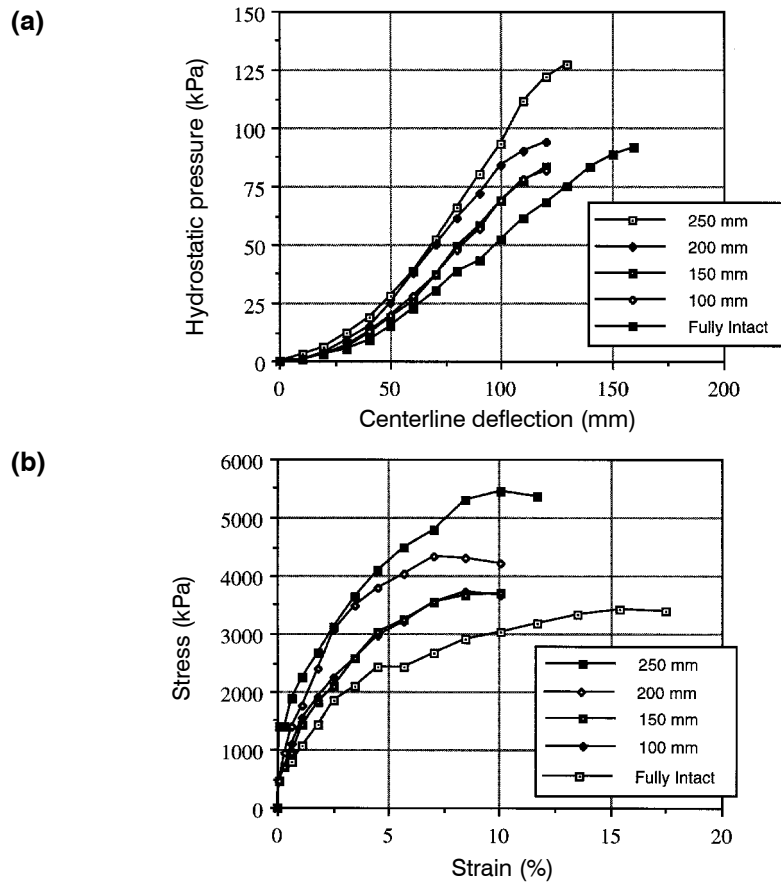


Figure 12. Comparison of test results for GCL-D1 specimens with different seam overlap length values: (a) raw data; (b) calculated stress versus strain data.

provides a larger amount of GCL edge support as the overlap distance becomes greater. A rectangular configuration (LaGatta 1992; Boardman 1993) would be more representative of the field loading condition.

While these comments challenge the validity of this type of overlap seam setup, the tests do suggest that the overlap seams *from a strength perspective* do not appear to be a concern.

5 SUMMARY AND CONCLUSIONS

This paper presents the three-dimensional, axi-symmetric tension behavior of ten GCL products manufactured by five different manufacturers. To the authors' knowledge the test method has not been used previously to evaluate GCLs. A VLDPE geomembrane was used in these tests to provide a watertight pressurizing layer above the

GCL specimens. Other candidate geomembranes for this purpose are linear low density polyethylene (LLDPE), flexible polypropylene (fPP) and polyvinyl chloride (PVC).

Before making comparisons and generalizations, however, it must be emphasized that GCL manufacturing is in a constant state of evolution. At least three of the products listed in Table 2 are no longer commercially available and all GCL manufacturers have modified their products and new products are appearing on the market on a regular basis. With the above caution in mind, Table 3 presents a summary of results for pressure and deflection at failure, as well as stress and strain at failure.

The following conclusions from the test results can be made:

- There is a general trend for the geotextile GCL specimens to be somewhat stronger than the geomembrane GCL specimens.
- Conversely, the geomembrane GCL specimens are considerably stiffer in their initial response as is expected for an HDPE geomembrane prior to yield.
- The failure strain of all GCL specimens ranged from 10 to 22%. This is of interest since the out-of-plane hydraulic conductivity studies reported by LaGatta (1992) and Boardman (1993) showed permeability breakthrough after an applied strain in the range of 10 to 15% for the geotextile related GCL products that were tested. By inference, it appears that hydraulic flow through the deformed geotextile type GCL specimens occurs slightly before the geosynthetic carrier layers fail from excessive deformation.
- Since there appears to be a slight extensibility in the geosynthetics beyond permeability breakthrough, the geosynthetic carrier layers may provide some protection against the loss of bentonite to underlying drainage layers. If this is the case, the geotextiles (or geomembranes) can be considered as containment layers against the loss of bentonite.
- The modes of failure of the different GCL specimens are listed in Table 3. All of the geotextile GCL specimens failed by tearing, while the geomembrane GCL specimens failed by centralized bursting.

Table 3. Three-dimensional, axi-symmetric results of GCL specimens evaluated in this study.

GCL number	Failure pressure (kPa)	Failure stress (kPa)	Failure deflection (mm)	Failure strain (%)	Mode of failure*	Figure number
A1	91	2500	150	15	2	6
A2	118	3600	160	17	2	6
B	~50	~2100	~120	~10	3	8
C	86	3200	170	19	2	9
D1	94	3500	160	17	1	10
D2	92	3300	170	19	1	10
D3	81	3300	140	13	1	10
E1	44	1700	170	22	4	11
E2	~45	~2000	~150	~15	4	11
E3	63	2700	130	15	4	11

Notes: *1 = tear in machine direction; 2 = tear in cross-machine direction; 3 = T-shaped tears in perpendicular directions; and 4 = centralized burst.

- Some of the geotextile GCL specimens failed (tore) in the machine direction, others tore in the cross-machine direction and one failure was T-shaped. The strength of the geotextile at the bottom of the GCL test specimen dictates the type of failure pattern.

In summary, it is felt that this study suggests the appropriateness of using geosynthetic clay liners (GCLs) in cases of localized, or differential settlement. As such, it complements and confirms the work of LaGatta (1992) and Boardman (1993) which was based on hydraulic considerations, as opposed to this study which is based on out-of-plane tensile strength and deformation considerations. While the application of this information to landfill covers is of major importance, the phenomenon can also occur elsewhere as was mentioned in the introduction.

Comparison of the out-of-plane tensile behavior of GCLs to compacted clay liners (CCLs), has shown that strains at failure for GCLs ranged from 10 to 22%, and were less than 1% for CCLs. It is felt that GCLs should be considered as being superior to CCLs if a natural soil material is desired as the barrier material to liquid flow when differential settlement is expected.

With respect to a comparison of the out-of-plane tensile behavior of GCL specimens to geomembranes (which use precisely the same test method), this data indicates that GCLs are similar to some geomembranes (such as CSPE-R and HDPE), but are not as flexible as other geomembranes such as VLDPE, LLDPE, fPP and PVC. This leads to the conclusion that if a *composite* liner is required in an application which may undergo differential settlement the recommended composite liner choices are VLDPE/GCL, LLDPE/GCL, fPP/GCL or PVC/GCL.

ACKNOWLEDGMENT

This project was funded by the Geosynthetic Research Institute which is a research and development consortium located at Drexel University in Philadelphia, Pennsylvania, USA.

REFERENCES

- ASTM D 5199, “*Standard Test Method for Measuring Nominal Thickness of Geotextiles and Geomembranes*”, American Society for Testing and Materials, West Conshohocken, Pennsylvania, USA.
- ASTM D 5617, “*Test Method for Multi-Axial Tension Test for Geosynthetics*”, American Society for Testing and Materials, West Conshohocken, Pennsylvania, USA.
- Boardman, B. T., 1993, “*The Potential Use of Geosynthetic Clay Liners as Final Covers in Arid Regions*”, M.Sc. Thesis, University of Texas, Austin, Texas, USA, 109 p.
- GRI GM4, 1993, “*Standard Test Method for Three Dimensional Geomembrane Tension Test*”, Geosynthetic Research Institute, Philadelphia, Pennsylvania, USA.

- Koerner, R.M. and Daniel, D.E., 1994, "Technical Equivalency Assessment of GCLs to CCLs", *Geosynthetic Liner Systems: Innovations, Concerns and Designs*, Koerner, R.M. and Wilson-Fahmy, R.F. Editors, IFAI, 1994, proceedings of a conference held in Philadelphia, Pennsylvania, USA, pp. 265-285.
- Koerner, R.M., Gartung, E. and Zanzinger, H., 1994, "Geosynthetic Clay Liners", Balkema, Rotterdam, 245 p.
- Koerner, R.M., Koerner, G.R. and Hwu, B.L., 1990, "Three Dimensional, Axi-Symmetric Geomembrane Tension Test", *Geosynthetic Testing for Waste Containment Applications*, Koerner, R.M., Editor, ASTM Special Technical Publication 1081, proceedings of a symposium held in Las Vegas, Nevada, USA, January 1990, pp. 170-184.
- LaGatta, M.D., 1992, "Hydraulic Conductivity Tests on Geosynthetic Clay Liners Subjected to Differential Settlement", M.Sc. Thesis, University of Texas, Austin, Texas, USA, 120 p.
- Steffen, H., 1984, "Report on Two-Dimensional Strain Stress Behavior of Geomembranes With and Without Friction", *Proceedings of the International Conference on Geomembranes*, IFAI, Vol. 1, Denver, Colorado, USA, June 1984, pp. 181-184.

ABBREVIATIONS

ASTM:	American Society for Testing and Materials
CCL:	compacted clay liner
CSPE-R:	reinforced chlorosulphonated polyethylene
fPP:	flexible polypropylene
GCL:	geosynthetic clay liner
GRI:	Geosynthetic Research Institute
HBNW-GT:	heat-bonded nonwoven geotextile
HDPE:	high density polyethylene
HDPE-GM(s):	high density polyethylene geomembrane (smooth)
HDPE-GM(t):	high density polyethylene geomembrane (textured)
K-GT:	knitted geotextile
LLDPE:	linear low density polyethylene
NPNW-GT:	needle-punched nonwoven geotextile
PVC:	polyvinyl chloride
SFW-GT:	slit-film woven geotextile
VLDPE:	very low density polyethylene